LAWRENCE
LIVERMORE
NATIONAL
LABORATORY

LLNL-TR-650567

TORUS Annual Continuation and Progress Report

G. Arbanas, C. Elster, J. Echer, F. Nunes, I. Thompson

February 25, 2014

Disclaimer

This work performed under the auspices of the U.S. Department of Energy by Lawrence Livermore National Laboratory under Contract DE-AC52-07NA27344.

Office of Science, U.S. Department of Energy
Office of Nuclear Physics
Nuclear Theory Division

TORUS:
Theory of Reactions for Unstable iSotopes

A Topical Collaboration for Nuclear Theory
Project Period: June 1, 2010 – May 31, 2015

Annual Continuation and Progress Report
Year-3: March 1, 2013 – February 28, 2014

Prepared by the TORUS Collaboration:

Goran Arbanas

Charlotte Elster

Jutta Escher

Filomena Nunes

Ian Thompson (Coordinating P.I.)

February 24, 2014

LLNL-TR-000000

Contents

1 Introduction

Background

The TORUS collaboration derives its name from the research it focuses on, namely the **T**heory **o**f **R**eactions for **U**nstable i**S**otopes. It is a Topical Collaboration in Nuclear Theory, and funded by the Nuclear Theory Division of the Office of Nuclear Physics in the Office of Science of the Department of Energy. The funding supports one postdoctoral researcher for the years 1 through 4. The collaboration brings together as Principal Investigators a large fraction of the nuclear reaction theorists currently active within the USA.

Mission

The mission of the TORUS Topical Collaboration is to develop new methods that will advance nuclear reaction theory for unstable isotopes by using three-body techniques to improve direct-reaction calculations. This multi-institution collaborative effort is directly relevant to three areas of interest: the properties of nuclei far from stability; microscopic studies of nuclear input parameters for astrophysics, and microscopic nuclear reaction theory.

Highlights from Year 4

1. Completed work on the Coulomb distorted form factors, publications [32, 33].
2. Separable potentials for neutron scattering off closed shell nuclei, publication [16].
3. Partial-wave coulomb wave functions in momentum space, paper submitted [10].
4. Determination of surface-operator contributions to bound and resonant states, paper submitted [12].
5. First self-consistent computation of direct neutron capture cross section for heavy deformed nuclei in a coupled-channel formalism for both initial and final states.
6. 9 papers published and another 7 submitted – Section 6.
7. 26 presentations, including invited talks at various national and international venues, such as the European Conference on Few-Body Problems in Physics – Section 6.3.

2 Research

2.1 Overview

The original budget for Ohio University of $11K is increased by $25K in order to accommodate the support of postdoctoral researcher Vasily Eremenko for three months (June, July, and August 2014). Starting Sepember 1, 2014, Eremenko will be postdoctoral researcher with the Nuclear Theory Group at Ohio University.

	Date of Plan		
Institution	Feb 2012	Feb 2013	Feb 2014
LLNL	$117k	$106k	$106k
MSU	$14k	$13k	$7k
TAMU	$27k	$25k	$24k
ORNL	$40k	$36k	$36k
Ohio	$11k	$10k	$36k
Total	$209k	$190k	$209k

Table 1: Budget requests for TORUS Year 5 (June 2014 – May 2015, incl.) as planned previously and currently.

2.2 Coupled-channel Theory

2.2.1 Revisiting surface-integral formulations for one-nucleon transfers to bound and resonance states

J.E. Escher and I.J. Thompson

We expanded our investigations of the surface-integral formalism that was proposed recently [20] to address shortcomings in the description of transfers to resonance states.

The surface-integral method builds on ideas from the very successful R-matrix theory; it uses a similar separation of the parameter space into interior and exterior regions, and introduces a parameterization that can be related to physical observables, which, in principle, makes it possible to extract meaningful spectroscopic information from experiments. The reaction amplitude is recast in terms of a surface integral plus remnant terms that contain contributions from the interior and exterior of the final nucleus, where interior and exterior are defined with respect to the distance r_{nA} between the transferred nucleon and the target nucleus: $M^{(DWBA)} = M^{(post)}_{\rm int}(0,a) + M_{\rm surf}(a) + M^{(prior)}_{\rm ext}(a,\infty)$. The notation $M(x,y)$ indicates the lower (x) and upper (y) limits of the integration over r_{nA}, and the surface term is evaluated at $r_{nA} = a$; 'post' and 'prior' refer to the standard post and prior formalisms used in transfer calculations. The interior post term is model-dependent, while the exterior prior and surface terms are related to the asymptotic properties of the wave function.

Previously, we had studied the contributions from the interior-post, surface, and exterior-prior terms to the (d,p) cross sections for several target nuclei in the DWBA framework. In all cases,

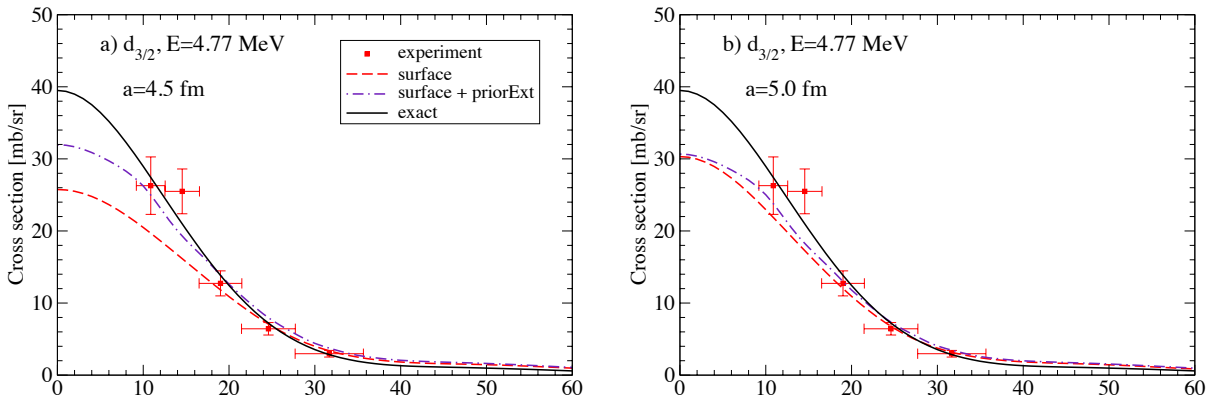

Figure 1: Surface-integral description of one-nucleon transfer to a $3/2^+$ resonance in ^{21}O. Improvements to the surface-term-only approximation can be achieved by including contributions from the prior-exterior term and selecting a small surface radius. Shown are the surface-only results (dashed curve) and the surface plus interior-prior results (dash-dotted curve), compared to the full calculation (solid line) and to experiment. The calculations in panel b) were carried out at a surface radius $a = 5.0$ fm that coincides with the maximum of the surface term, and panel a) shows the effect of reducing a by 0.5 fm. The cross section arising from the surface term decreases, while the cross section associated with the sum of the surface and the prior-exterior term shows improved agreement with the exact results.

for both bound and resonance final states, we had found that the surface term gives the dominant contributions, provided a separation radius is chosen that is in the region of the nuclear surface. When comparing to exact calculations of the cross sections, however, we also found that significant strength is missing (30-50%), which indicates that the residual terms cannot be neglected. In the region where the surface cross section peaks, we found contributions from both the interior-post and the exterior-prior terms.

Recently, we identified a path forward for practical applications of the surface-integral formalism. We considered a separation radius a that is slightly smaller than the radius corresponding to the peak of the surface term. This minimizes contributions from the post-interior term, thus removing the need for a model for the one-nucleon overlap function in the nuclear interior. With a decrease in the surface radius comes an increase in the contribution from the prior-exterior term, making it necessary to including this term explicitly. We illustrate the effect in Figure 1, where we consider a $3/2^+$ resonance at 4.77 MeV in ^{21}O. The surface cross section shown in panel b) was calculated with separation radius $a = 5.0$ fm, which corresponds to the maximum of the surface contribution. The curve falls clearly short of reproducing the full cross section. Also shown is a calculation that contains both surface and prior-exterior contributions. We observe a slight improvement in the agreement with the exact calculation, but additional contributions (from the post-interior term) would be needed to achieve satisfactory agreement.

Moving the separation radius to smaller values, however, improves the situation, as a comparison between panels a) and b) demonstrates. In panel a) we show analogous surface-only and surface-plus-interior-prior calculations, but for a radius that is 0.5 fm smaller than in panel b). While this shift in a reduces the surface-only cross section, it increases the cross section arising from the the exterior-prior term, with the sum giving a much better approximation to the exact cross section. Similar results were found for a $3/2^+$ and a $7/2^-$ resonance at 6.17 MeV.

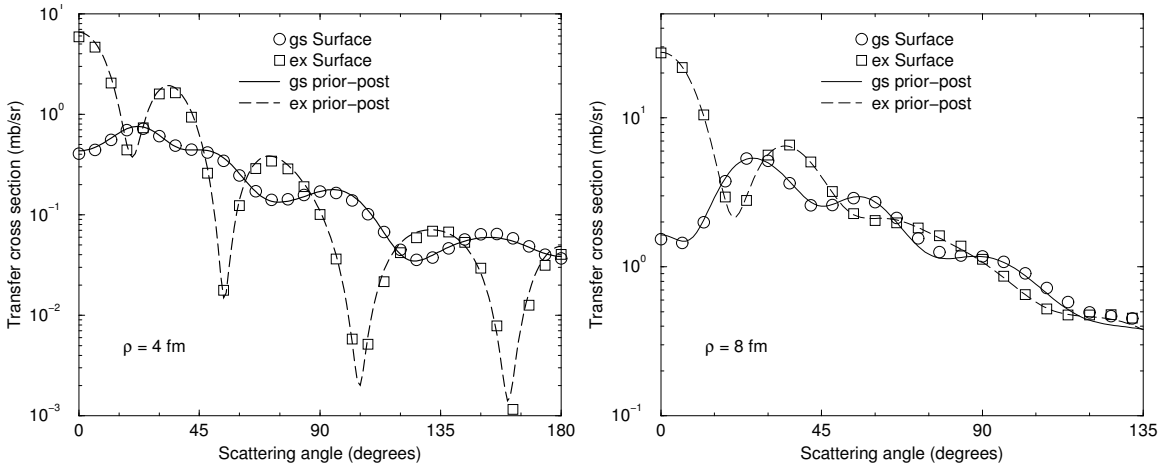

Figure 2: Comparison of methods to calculate the surface transfer contribution, for the ^{90}Zr(d,p) reaction at deuteron energy of 11 MeV. On the left the surface radius is $a = 4$ fm, and on the right 8 fm. The gs is a $d_{5/2}$ neutron state, and the excited state is a $s_{1/2}$ state.

A paper summarizing these results has been submitted to Physical Review C [12]. Our findings are significant, as they point to likely improvements of the surface-integral approach when implemented in the continuum-discretized coupled-channels (CDCC) framework [1]. In the CDCC framework one-neutron transfers and deuteron breakup are treated simultaneous and, according to Ref. [20], the exterior-prior term no longer appears, *i.e.* $M^{CDCC} = M^{CDCC}_{\rm int}(0,a) + M^{CDCC}_{\rm surf}(a)$.

Year 5 plan: We will extend our studies to the CDCC approach, using the newly-implemented CDCC surface-operator described in Section 2.2.2 below. Specifically, we will determine the surface and breakup contributions in measured stripping cross sections.

2.2.2 Surface transfer operator for general use

I.J. Thompson

In order to calculate transfer cross sections with the surface operator at some final neutron radius $r' = a$, we have to implement the general surface operator, not just its value of the 'prior–post' difference, as used in the previous section 2.2.1. The needed source term $S^{\rm surf}_{\beta\alpha}(R')$ in a final (proton) channel β from the initial (deuteron) channel α is, with the surface operator,

$$S^{\rm surf}_{\beta\alpha}(R') = \langle Y_\beta(\hat{R}',\hat{r}')\Phi_\beta(r')|\overleftarrow{T_{nA}} - \overrightarrow{T_{nA}}|\Phi_\alpha(r)\,Y_L(\hat{R})u_\alpha(R)\rangle_{r'>a} \quad (1)$$

$$= \frac{-\hbar^2}{2\mu_n}\int_0^\infty dr' \left\langle Y_\beta(\hat{R}',\hat{r}')\Big|\delta(r'-a)\left[\frac{\partial\Phi_\beta(r')}{\partial r'} - \Phi_\beta(r')\frac{\partial}{\partial r'}\right]\Big|\Phi_\alpha(r)Y_L(\hat{R})\right\rangle u_\alpha(R) \quad (2)$$

where Φ_β is the final state of the neutron, whether bound or unbound. This coupling is non-local as $R' \neq R$, and depends on the derivatives of the deuteron incoming wave function $u_\alpha(R)$, so we need to calculate the two non-local kernel functions $\mathsf{X}_{\beta\alpha}(R',R)$ and $\mathsf{Y}_{\beta\alpha}(R',R)$ to give the source term as

$$S^{\rm surf}_{\beta\alpha}(R') = \int_0^\infty dR\,\mathsf{X}_{\beta\alpha}(R',R)u_\alpha(R) + \int_0^\infty dR\,\mathsf{Y}_{\beta\alpha}(R',R)\left[u'_\alpha(R) - \frac{L_\alpha+1}{R}u_\alpha(R)\right] = 0\,. \quad (3)$$

The derivative operators in Eq. (2) operate on all of the radii r, R and their angles $\hat{r}, \hat{R}$, so X has four terms. Using the $\Phi_\alpha(r)$ and $\hat{\Phi}_\alpha(r) = \frac{1}{r}(\varphi'_\alpha(r) - \frac{\ell+1}{r}\varphi_\alpha(r))$ variables for both entrance and exit channels, kinematical coefficients a', b', p, P, J, and Clebsch-Gordan products $G^{\alpha'\alpha}_{m'_\ell M_L m_\ell}$, we have derived

$$
\begin{aligned}
X_{\alpha'\alpha}(R',R) = -J\frac{\hbar^2}{2\mu_n}\frac{a}{a'b'}\sum_{m'_\ell m_\ell}\sum_{M_L=-1}^{1} G^{\alpha'\alpha}_{m'_\ell M_L m_\ell}\, P^{|m'_\ell|}_{\ell'}(\cos\theta_{r'}) P^{|M_L+m_\ell-m'_\ell|}_{L'}(\cos\theta_{R'})
\\
\Bigg[\ \Phi'_\beta(a)\, Y^{M_L}_L(\hat{\mathbf{R}})\, Y^{m_\ell}_\ell(\hat{\mathbf{r}})\Phi_\alpha(r)
\\
- \Phi_\beta(a)\, Y^{M_L}_L(\hat{\mathbf{R}})\frac{p}{r}\sqrt{\frac{4\pi\ell(2\ell+1)}{3}}\sum_{\lambda=-1}^{1}\langle \ell{-}1\ m_\ell{-}\lambda, 1\lambda|\ell m_\ell\rangle Y^{m_\ell-\lambda}_{\ell-1}(\hat{\mathbf{r}})Y^{\lambda}_1(\hat{\mathbf{r}'})\Phi_\alpha(r)
\\
- \Phi_\beta(a)\, Y^{M_L}_L(\hat{\mathbf{R}})p\ \hat{\mathbf{r}}\cdot\hat{\mathbf{r}'}\ Y^{m_\ell}_\ell(\hat{\mathbf{r}})\hat{\Phi}_\alpha(r)
\\
- \Phi_\beta(a)\, Y^{m_\ell}_\ell(\hat{\mathbf{r}})\Phi_\alpha(r)\ \frac{P}{R}\sqrt{\frac{4\pi L(2L+1)}{3}}\sum_{\Lambda=-1}^{1}\langle L{-}1\ M_L{-}\Lambda, 1\Lambda|LM_L\rangle Y^{M_L-\Lambda}_{L-1}(\hat{\mathbf{R}})Y^{\Lambda}_1(\hat{\mathbf{r}'})\Bigg],
\end{aligned}
\tag{4}
$$

and the derivative term (with $M_L = 0$):

$$
\begin{aligned}
Y_{\alpha'\alpha}(R',R) =& J\frac{\hbar^2}{2\mu_n}\frac{a}{a'b'}P\Phi_\beta(a)\Phi_\alpha(r)\ \ \hat{\mathbf{R}}\cdot\hat{\mathbf{r}'}
\\
&\times\sum_{m'_\ell m_\ell} G^{\alpha'\alpha}_{m'_\ell 0 m_\ell} P^{|m'_\ell|}_{\ell'}(\cos\theta_{r'}) P^{|m_\ell-m'_\ell|}_{L'}(\cos\theta_{R'})\ Y^{m_\ell}_\ell(\hat{\mathbf{r}})Y^0_L(\hat{\mathbf{R}}).
\end{aligned}
\tag{5}
$$

These expressions (4) and (5) have been directly implemented in a LLNL version of our coupled-channels code FRESCO [29]. This is the first time that derivatives of scattering wave functions have been needed. The results have been validated by comparison with the angular cross sections obtained in the work described in the previous section 2.2.1. The comparisons are shown in Figure 2.

2.2.3 Integration of direct and compound reactions

J. Escher, in collaboration with experimentalists from U Richmond and LLNL

The interplay of direct and compound mechanisms in one-nucleon transfer reactions is of interest to the TORUS collaboration. J. Escher has been working with experimental colleagues from the University of Richmond and from LLNL to study one-nucleon (p,d) transfer reactions that produce intermediate nuclei at excitation energies near and above the particle thresholds. Measurements, carried out Lawrence Berkeley Laboratory and at the Texas A&M Cyclotron Laboratory, for (p,d) reactions on gadolinium, yttrium, and zirconium nuclei, have generated new insights into shell structure and the interplay of direct and compound-nuclear processes [26, 17].

J. Escher, in collaboration with theorists from Sao Paulo, Brazil

In collaboration with Mahir Hussein (Universidade de São Paulo, Brazil) and Brett Carlson (São José dos Campos, SP, Brazil), J. Escher has been revisiting the present status of theoretical

descriptions of compound-nuclear reactions. An invited paper for a special volume on Open Problems in Nuclear Reaction Theory is nearing completion and will be submitted to Journal of Physics G.

2.3 Faddeev Theory

2.3.1 Coulomb in momentum space without screening

Upadhyay and Nunes, in collaboration with OU

One of the most challenging aspects of solving the three-body problem for nuclear reactions is the repulsive Coulomb interaction. While for light nuclei, often the Coulomb interaction is a small correction to the problem, this is certainly not the case for intermediate mass and heavy systems [22]. Over the last decade many theoretical efforts have focused on advancing the theory for (d,p) (e.g. [19, 3]) and testing existing methods (e.g. [7, 31]). Currently, the most complete implementation of the theory is provided by the Lisbon group [4], which solves the Faddeev equations in momentum space written in the plane wave basis (the so-called AGS equations for Alt, Grassberger and Sandhas). The method introduced in [4] treats the Coulomb interaction with a screening and renormalization procedure as detailed in [6, 5]. While the current implementation of the AGS with screening is computationally effective for light systems, as the charge of the nucleus increases, technical difficulties arise in the screening procedure [22]. Indeed, for most of the new exciting nuclei to be produced at the Facility of Rare Isotope Beams, the current method is not adequate. One then has to explore solutions to the nuclear reaction three-body problem where Coulomb is treated without screening.

This is precisely what is done in [19]. Mukhamedzhanov *et al.* derived a theory for (d,p) whereby the AGS equations are casted in the Coulomb distorted wave representation, instead of the plane wave basis. For a practical implementation of the theory of [19], one needs to be able to accurately compute the Coulomb distorted form factors used as a basis for the theory. This was the focus of the MSU activities during 2013.

A closed analytic form for the Coulomb function in momentum space was first derived in [8]. The procedure starts with the Fourier transform of the Coulomb wave function in coordinate space:

$$\Psi^C_{\mathbf{p}}(\mathbf{q}) = -4\pi \exp^{-\eta\pi/2} \Gamma(1+i\eta) \lim_{\gamma\to+0} \frac{d}{d\gamma} \left\{ \frac{[q^2-(p+i\gamma)^2]^{i\eta}}{[\gamma^2+(\mathbf{p}-\mathbf{q})^2]^{1+i\eta}} \right\}. \tag{6}$$

Next, one performs the partial wave decomposition, and after some non-trivial mathematical manipulations, obtains the expression:

$$\psi^C_{l,p}(q) \;=\; -\frac{2\pi\, e^{\eta\pi/2}}{pq} \lim_{\gamma\to+0} \frac{d}{d\gamma} \left\{ \left[\frac{q^2-(p+i\gamma)^2}{2pq} \right]^{i\eta} (\zeta^2-1)^{-i\frac{\eta}{2}}\, Q_l^{i\eta}(\zeta) \right\} . \tag{7}$$

Here p is the magnitude of a fixed asymptotic momentum and $\zeta = (p^2+q^2)/2pq$. The Sommerfeld parameter is given as $\eta = Z_1 Z_2 e^2 \mu/p$ with $Z_1 Z_2 e^2$ being the total charge and μ the reduced mass of the two-body system under consideration. The spherical function $Q_l^{i\eta}(\zeta)$ is expressed in terms

of Hypergeometic functions ${}_2F_1$, depending on angular momentum l, the strength of the Coulomb potential η and the dynamic variable related to the momenta $\zeta = (p^2+q^2)/2pq$:

$$\begin{aligned} Q_l^{i\eta}(\zeta) &= \frac{e^{-\pi\eta}}{2}\Bigg\{\Gamma(i\eta)\,\left(\frac{\zeta+1}{\zeta-1}\right)^{\frac{i\eta}{2}}\,{}_2F_1\left(-l,l+1;\,1-i\eta;\,\frac{1-\zeta}{2}\right) \\ &\quad +\Gamma(-i\eta)\,\frac{\Gamma(l+1+i\eta)}{\Gamma(l+1-i\eta)}\,\left(\frac{\zeta-1}{\zeta+1}\right)^{\frac{i\eta}{2}}\,{}_2F_1\left(-l,l+1;\,1+i\eta;\,\frac{1-\zeta}{2}\right)\Bigg\}. \end{aligned} \quad (8)$$

These ${}_2F_1$ have tricky conditions, and are hidden in the spherical function $Q_l^{i\eta}$. The spherical functions in Eq. (8) are valid under two conditions: (a) $|\arg(\zeta\pm1)| < \pi$ and (b) $|1-\zeta| < 2$, *i.e.*, $-1 < \zeta < 3$. Since ζ is a positive quantity, it always satisfies condition-(a). However, condition-(b) is in some physical situations not satisfied, giving rise to spurious behavior of the function in the region outside the valid range, namely when p is very small or very large. In those situations we have to consider alternate expansions.

The $Q_l^{i\eta}(\zeta)$ can also be expanded for $|\zeta| > 1$ as:

$$Q_l^{i\eta}(\zeta) = \frac{e^{-\pi\eta}\Gamma(l+i\eta+1)\Gamma(\frac{1}{2})}{2^{l+1}\,\Gamma(l+\frac{3}{2})}\,\frac{(\zeta^2-1)^{\frac{i\eta}{2}}}{\zeta^{l+i\eta+1}}\,{}_2F_1\left(\frac{l+i\eta+2}{2},\,\frac{l+i\eta+1}{2};\,l+\frac{3}{2};\,\frac{1}{\zeta^2}\right). \quad (9)$$

Eq. (9) is well-behaved at low and high momenta, where the original expression Eq. (8) is ill defined. Eq. (8) is valid around the singularity. Thus, it is important to switch to the appropriate expansion depending on the value of ζ.

The Coulomb distorted form factors, needed for the Faddeev AGS equations for a three-body system consisting of a deuteron and a nucleus [19], for which the interactions are given as separable forces of arbitrary rank, are integrals over a nuclear formfactor $u_l(q)$ and the Coulomb wave function $\psi^C_{l,p}(q)$

$$u_l^C(p) = \int_0^\infty \frac{dq\;q^2}{2\pi^2}\;u_l(q)\;\psi^C_{l,p}(q)^\star. \quad (10)$$

The nuclear formfactors should be chosen according to the physical properties of the two-body system under consideration. While for the neutron-proton interaction traditionally a superposition of Yamaguchi formfactors is used [14], for the interaction between neutrons or protons and a nucleus, separable forms of phenomenological optical potentials [16] should be employed. Our formulation for calculating the integrals of Eq. (10) is general. For the sake of numerically testing our approach we will present calculations based on Yamaguchi-type formfactors in Section 2.3.2.

The main challenge in computing the integral of Eq. (10) is its oscillatory singularity for $p = q$, of the form

$$S(p-q) = \lim_{\gamma\to+0}\frac{1}{(p-q+i\gamma)^{1+i\eta}}. \quad (11)$$

This type of singularity cannot be numerically evaluated by familiar principal value subtractions but rather needs to be treated using the scheme proposed by Gel'fand and Shilov [13]. The essence of this scheme is to subtract as many terms as needed of the Laurent expansion in a small region around the pole so that the oscillations around the pole become small, and the value of the integral around the pole can be estimated analytically.

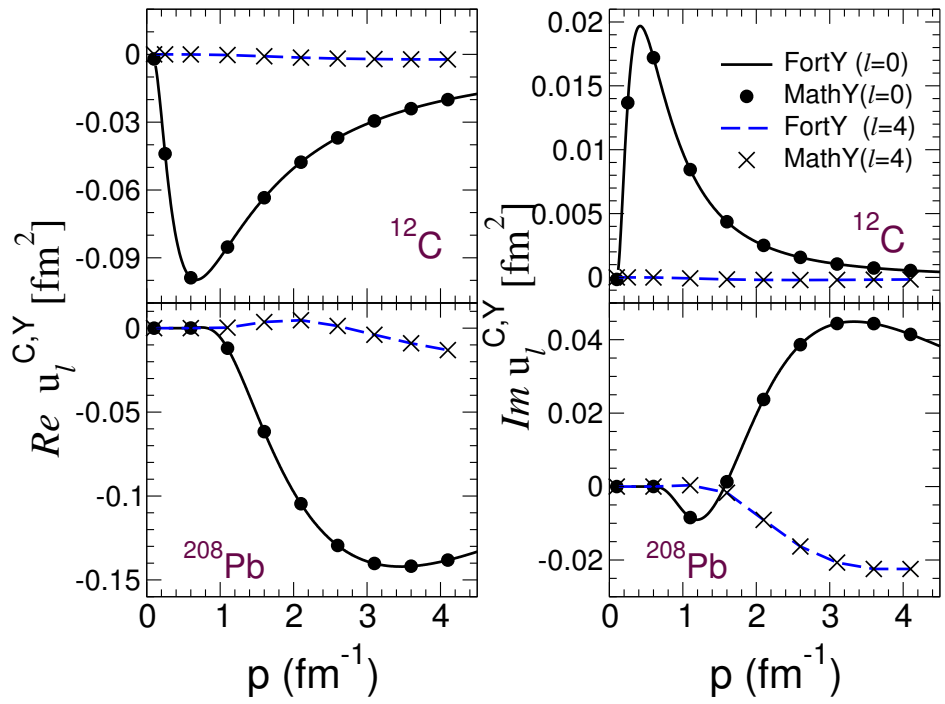

Figure 3: The partial wave Coulomb formfactors $u_l^C(p)$ obtained with a Yamaguchi interaction as a function of the external momentum p for selected angular momenta l. Comparison between our numerical evaluation (solid lines) and the *Mathematica*® [25] results (symbols).

To our knowledge, this work represents the first attempt to numerically obtain matrix elements with relatively high values of charges involved in the Coulomb distorted basis in momentum space. Given the challenge of accurately calculating the partial wave Coulomb wave functions as well as handling their oscillating singularity, it is critical to demonstrate the numerical accuracy of our computations $u_l^C(p)$ of Eq. (10). For this reason we first study the Coulomb distorted nuclear formfactors for the separable Yamaguchi interaction as used in Refs. [19].

2.3.2 Tests with a Yamaguchi Formfactor

Upadhyay and Nunes, in collaboration with OU

Using a Yamaguchi formfactor as a test case has the advantage that calculations can be performed not only numerically but also semi-analytically, in our case using the *Mathematica* ® [25] software. The Coulomb distorted formfactors, $u_l^{C,Y}(p)$ calculated as integral over the Coulomb wave function given in Eq. (7) and the Yamaguchi formfactor from [19] are depicted in Fig. 3, where our numerical results (labeled FortY) are compared with those from *Mathematica* ® [25] (labeled MathY). The top panels concern protons on ^{12}C and the bottom panels refer to protons on ^{208}Pb. On the right (left) we show the real (imaginary) parts of $u_l^{C,Y}(p)$. Both $l = 0$ and $l = 4$ are shown.

As shown in Fig. 3, the Coulomb distorted Yamaguchi formfactors obtained with our numerical implementation agree perfectly well with the results obtained with *Mathematica*®. To achieve this

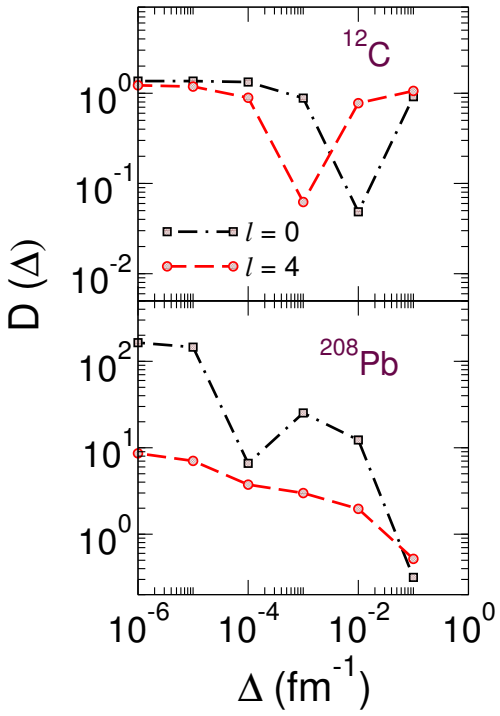

Figure 4: The relative difference $\mathbf{D}(\Delta)$ of the exactly calculated integral of Eq. (10) and the integral without including the region $\pm\Delta$ around the pole as a function of Δ for p+^{12}C at $p = 0.6$ fm^{-1} (top) and p+^{208}Pb at $p = 1.1$ fm^{-1} (bottom). Shown are l=0 (dot-dashed) and l=4 (dashed) partial waves.

level of agreement in the form factors, we first compared the accuracy of our numerical implementation of the Coulomb wave functions with the corresponding results provided by *Mathematica*®. The agreement found was in the order of 10 significant figures. Next, we compared the accuracy of the integration given by Eq. (10) and found that our numerical calculation agreed with the corresponding *Mathematica*® calculation for about 6 significant figures. This demonstrates that our numerical implementation of the Coulomb wave functions, integration and regularization techniques provides a reliable method for calculating form factors involving Coulomb wave functions in momentum space.

In order to explore the importance of the region around the singularity, we have performed additional calculations where we removed a region $p \in [q - \Delta, q + \Delta]$ around the pole $p = q$ from the integral of Eq. (10). In Fig. 4 we show the absolute value of the relative difference between the results $u_l^{C,Y}(p, \Delta)$, obtained removing the pole region, and the full integral $u_l^{C,Y}(p)$, i.e. the quantity

$$\mathbf{D}(\Delta) = \frac{|u_l^{C,Y}(p) - u_l^{C,Y}(p, \Delta)|}{|u_l^{C,Y}(p)|} \tag{12}$$

for fixed values of q. We choose $p = 0.6$ fm^{-1} ($E_{c.m.} = 8.1$ MeV) for ^{12}C and $p = 1.1$ fm^{-1} ($E_{c.m.} = 7.5$ MeV) for ^{208}Pb, as examples. For each of these values of p the nuclear formfactor is far from any node. In Fig. 4 the calculations of the above defined quantity $\mathbf{D}(\Delta)$ are shown as function of Δ for p+^{12}C in panel (a), and for p+^{208}Pb in panel (b) for the $l = 0$ (dot-dashed lines) and $l = 4$ (dashed lines). In case of ^{12}C we find that the relative difference is always around 10%

or larger, independent of the Δ used and independent of the partial wave. Expectedly, the situation for ^{208}Pb is worse, discrepancies are about two orders of magnitude for $l = 0$ and one order of magnitude for $l = 4$. The demonstration given in Fig. 4 emphasizes the importance of the pole region.

Section 2.3.5 will show computations the $u_l^{C,Y}(p)$ form factors for realistic interactions, namely the separable forms developed by [16] and described next.

2.3.3 Separable representation of phenomenological optical potentials of Woods-Saxon type

Hlophe and Elster

One important ingredient for many applications of nuclear physics to astrophysics, nuclear energy, and stockpile stewardship are cross sections for reactions of neutrons with rare isotopes. Since direct measurements are often not feasible, indirect methods, e.g. (d,p) reactions, should be used. Those (d,p) reactions may be viewed as three-body reactions and described with Faddeev techniques. Faddeev equations in momentum space have a long tradition of utilizing separable interactions in order to arrive at sets of coupled integral equations in one variable. While there exist several separable representations for the nucleon-nucleon interaction, the optical potential between a neutron (proton) and a nucleus is not readily available in separable form. For this reason we introduced a separable representation for complex phenomenological optical potentials of Woods-Saxon type.

We extended the well-known EST scheme [11] for creating separable representations of two-body transition matrix elements as well as potentials to the realm of complex potentials. Requiring that the separable transition matrix fulfill the reciprocity theorem, we identified a suitable rank-1 separable potential. In analogy to Ref. [11], we generalized this potential to arbitrary rank.

Our calculations were based on the Chapel Hill phenomenological optical potential CH89 [34]. Since the CH89 potential, as nearly all phenomenological optical potentials, is given in coordinate space using Woods-Saxon functions, we first give a semi-analytic Fourier transform of those Woods-Saxon functions in terms of a series expansion. In practice, it turns out that only two terms in the expansion are sufficient for achieving convergence. Note that our approach for deriving the momentum-space optical potential is general and can be applied to any optical potential of Woods-Saxon form. This momentum space CH89 potential is then used in the partial-wave LS integral equation to calculate half-shell t-matrices. These then serve as input to the the generalized scheme for creating separable representations for complex potentials.

We carried out studies of n+^{48}Ca, n+^{132}Sn and n+^{208}Pb, and are able to provide for all cases a systematic classification of support points for partial-wave groups, so that the partial-wave S-matrices are reproduced to at least 4 significant figures compared to the original momentum space solution of the LS equation. We find the low partial waves of the n+^{208}Pb system require a rank-5 separable potential to be well represented in the energy regime between 0 and 50 MeV center-of-mass energy. The support points obtained for this case are well suited to represent all partial waves of the n+^{208}Pb as well as all lighter systems described by the CH89 optical potential.

We found that the rank required for achieving a good representation decreases with increasing angular momentum of the partial wave considered. We developed recommendations for both the rank and the locations of support points to be used when describing medium-mass and heavy

systems generated from the CH89 potential. Our recommendations group together partial waves. We also demonstrated that it is sufficient to determine support points including only the central part of the optical potential; when the spin-orbit interaction is added and the form factors are accordingly modified, the same support points can be expected to yield a good representation.

We then investigated the off-shell behavior of the constructed separable representations, and found that overall, the high momentum components along the $k = k'$ axis which are typical for local potentials are removed from the separable representation. Furthermore, the off-shell elements of the separable representation are smaller in magnitude, however follow the functional shape of the CH89 potential. Since off-shell matrix elements are not observables, only reaction calculations can show if the differences seen in the off-shell t-matrix have any consequences for e.g. three-body observables. Future work will have to address this question.

Our findings are published in *Physical Review C* [16].

2.3.4 Numerical Implementation of Momentum Space Partial Wave Coulomb Wave Functions

Eremenko and Elster, in collaboration with MSU

In order for the approach described in [21] to be numerically practical, one needs to have exact expressions for the Coulomb wave function in momentum space as well as reliable techniques to calculate expectation values in this basis.

A considerable amount of analytical studies and comparisons with the *Mathematica* ® [25] software were carried out by Upadhyay and Nunes, with further details being given in Section 2.3.2. Numerical implementation into robust a computational package and tests against the MSU results were carried out by Eremenko. This suite of codes evaluates the momentum space partial wave Coulomb wave functions for large range of Sommerfeld parameters ($10^{-1} \leq \eta \leq 10$) with a tested accuracy of about 10^{-6}.

The suite of codes together with a manuscript are currently under preparation for a submission to *Computer Physics Communication* [33], so that this work is available to other researchers. To our knowledge, there is nothing of this kind available in computational libraries.

2.3.5 Calculation of Coulomb matrix elements for separable optical potentials

Eremenko, Hlophe and Elster, in collaboration with MSU

After successfully establishing that we correctly implemented the regularization scheme proposed by Gel'fand and Shilov [13], we used the Woods-Saxon type formfactors, as derived in Ref. [16] and described in Section 2.3.3, for computing the form factors $u_l^C(p)$, after adjusting them to p+nucleus scattering,

In Fig. 5 we show in the left panels non-distorted formfactors from the separable optical potentials for n+^{12}C, n+^{48}Ca, and n+^{208}Pb. The right panels show the corresponding Coulomb distorted formfactors. At zero momentum, the nuclear formfactors are finite for $l = 0$ while going to zero as p^l for all higher angular momenta as dictated by the partial wave decomposition of the two-body t-matrix they are derived from. In contrast, the Coulomb distorted formfactors are also zero for

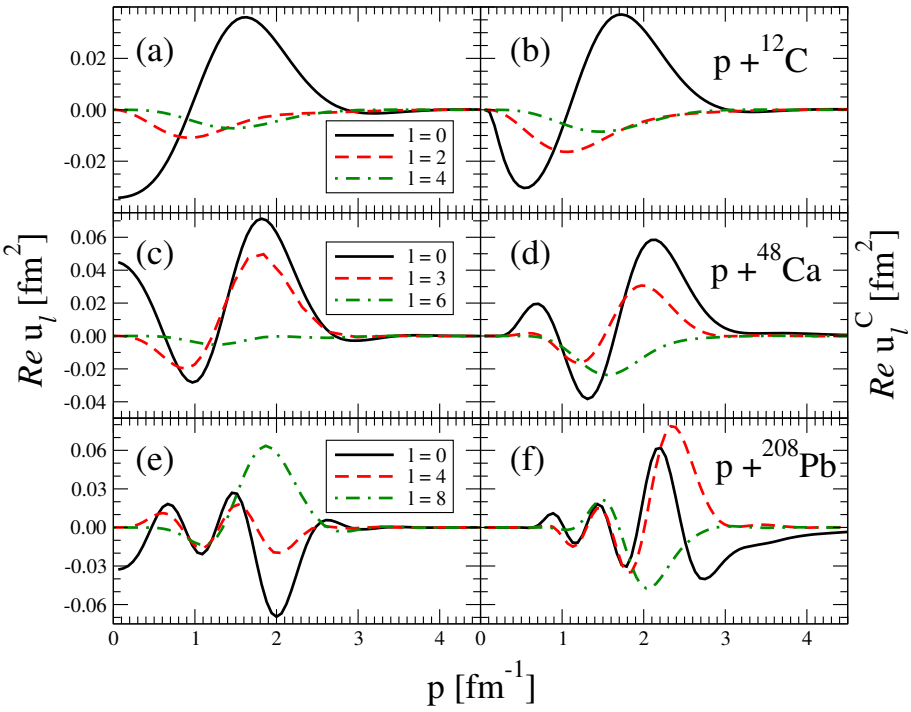

Figure 5: The real parts of the partial wave nuclear form factors $u_l(p)$ (left panels) and the Coulomb distorted nuclear form factors $u_l^C(p)$ (right panels) as function of the the external momentum p for selected angular momenta l: (a) $\Re e\, u_l(p)$ for n+^{12}C; (b) $\Re e\, u_l^C(p)$ for p+^{12}C; (c) $\Re e\, u_l(p)$ for n+^{48}Ca; (d) $\Re e\, u_l^C(p)$ for p+^{48}Ca. (c) $\Re e\, u_l(p)$ for n+^{208}Pb; (d) $\Re e\, u_l^C(p)$ for p+^{208}Pb. The formfactors for ^{12}C correspond to the fixed support point E_{cm} = 30 MeV, that for ^{48}Ca is at a fixed support point E_{cm} = 36 MeV, while the nuclear formfactors for ^{208}Pb are at a fixed support point E_{cm} = 36 MeV for $l = 0, 4$, and E_{cm} = 39 MeV for $l = 8$.

$l = 0$ at $p = 0$. This is associated with the existence of a repulsive barrier at the origin. Comparing the left and right panels of Fig. 5 also shows that the Coulomb interaction generally pushes the structure of the formfactors from lower momenta to higher momenta. In addition we observe that the heavier the nucleus, the more structure the corresponding formfactors exhibit. However, it is interesting to note, that for all nuclei under consideration the formfactor goes to zero already at 3 to 4 fm^{-1}, which is a property of the underlying Woods-Saxon ansatz.

In order to carefully study the role of the pole region in the integral of Eq. (10), we perform the integration, but leave out a region of momenta around the pole $p \in [q-\Delta, q+\Delta]$ when computing the integral. In Fig. 6 we compare the complete calculation of the real part of the $l = 0$ Coulomb distorted formfactor, $u_0^C(p)$, for ^{12}C with calculations of the same integral in which a region Δ around the pole at p was neglected. The complete calculation is the same as shown in Fig. 5. We find that for large Δ (say $\Delta = 0.1$ fm^{-1}) the formfactor has little resemblance with the exact one. As Δ becomes smaller, at least in the higher momentum region one can see a continuous build-up towards the exact result. In Fig. 7 we show the identical calculations for the real part of the $l = 0$ formfactor for the ^{208}Pb formfactor. Here we find that although for all values of Δ considered the formfactor computed without the pole region follows the shape of the full formfactor, it has quite

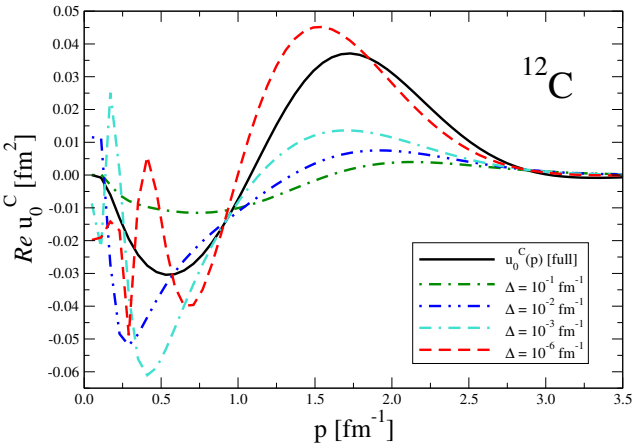

Figure 6: The real part of the $l = 0$ the Coulomb distorted nuclear formfactors $u_0^C(p)$ as function of the the external momentum p for ^{12}C at the fixed support point E_{cm} = 30 MeV. The solid (black) line shows the full results, while for all other curves an interval of the size Δ has been cut out left and right of the pole p while performing the integration.

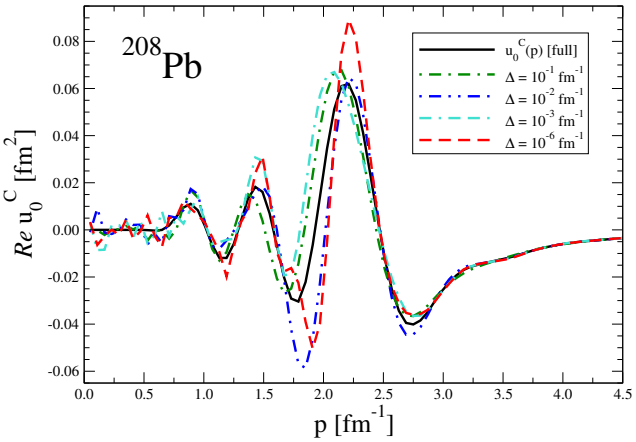

Figure 7: The real part of the $l = 0$ the Coulomb distorted nuclear formfactors $u_0^C(p)$ as function of the the external momentum p for ^{208}Pb at the fixed support point E_{cm} = 36 MeV. The solid (black) line shows the full results, while for all other curves an interval of the size Δ has been cut out left and right of the pole p while performing the integration.

different values.

To obtain some qualitative insight into this behavior, one has to have the functional form of the Coulomb wave function, $\psi_{l,p}^C(p')$, in mind and consider the dependence on the Sommerfeld parameter η. The smaller η, the more narrowly peaked around the pole p the Coulomb wave function becomes. In case of the ^{208}Pb formfactor calculation shown in Fig. 7, η is large and $\psi_{l,p}^C(p')$ has a relatively broad distribution around the pole at p. Consequently, in the integration a relatively large momentum interval of the nuclear formfactor $u_l(p')$ contributes. In the case of ^{12}C the Sommerfeld parameter η is already an order of magnitude smaller, and decreases further as function of p, making the momentum distribution of the Coulomb wave function much narrower. In the small p region of Fig. 6 only a relatively small momentum region of the smooth nuclear formfactor con-

tributes to the integral. For larger p the value of η becomes smaller and the momentum distribution of the Coulomb wave function even narrower, so that only a very restricted momentum region of the nuclear form factor contributes, leading to the appearance of an almost build-up to the final answer. The Coulomb wave functions contain as one of the leading terms the factor $\exp(-\pi\eta)$, see Eq. (8), thus for large values of η, the contributions in the integrand are smaller. This explains that the variations of the integral for small momenta p are much smaller for ^{208}Pb than for ^{12}C. For example, the value $\eta \sim 1.6$ occurs for ^{12}C at $p \simeq 0.12$ fm^{-1}, while for ^{208}Pb at $p \simeq 1.8$ fm^{-1}. For those momenta both figures show a strong variation of the integral as function of Δ. Once the momenta p become larger, η quickly becomes smaller. In summary, both of these demonstrations show that it is of uttermost importance to carefully treat the pole region in the integral of Eq. (10), since major contributions to this integral come from the region around the pole.

A manuscript showing our findings in detail is close to completion, and will be submitted to *Physical Review C* soon [33].

Plans for Year 5

We plan to have all manuscripts currently under preparation submitted within the next four weeks. Then we will fully concentrate on the work on the (d,p) reaction code based on the Faddeev-AGS formulation as outlined in Ref. [19]. Eremenko will take the lead in deriving the necessary expressions in a form which can be implemented into computer code. He will also take the lead in the code development, taking advantage of the computational infrastructure we developed in the past year. In this part of the development phase we will not yet implement target excitations, but plan the code structure already such that this can be added at a later stage,

During Year 5 OU and MSU will continue to work closely with regular meetings, to take advantage of the collective knowledge on reaction calculations within the collaboration.

Linda Hlophe decided to stay with the TORUS collaboration for his remaining thesis work. He will develop the separable coupling potentials needed to add core excitations to the EST formulation for separable optical potentials. It is planned that Nunes will provide additional guidance in this phase of the project.

Hlophe will further test his potentials containing core excitations within a Faddeev-AGS code containing only a small number of partial waves, but sufficiently general, that his work then can be merged with the work of Eremenko. The close collaboration with Nunes will be very beneficial for this part of the project.

Hlophe defended his Ph.D. prospectus containing these aspects of his future work in November 2014.

2.3.6 Other efforts

Nunes and others at MSU

The work of the TORUS postdoc, Neelam Upadhyay, in close collaboration with the OU team, have been the central contribution of MSU to TORUS. However, there are other projects, that connect to the research developed in TORUS, and that provide leverage to TORUS. Below we

provide a short list of those efforts:

- Luke Titus, an MSU PhD student, in collaboration with Nunes, have been investigating nucleon-nucleus non-local potentials. Titus has developed a code to solve the scattering problem with non-local interactions (manuscript submitted) and is developing the formalism to be able to include non-local interaction in the calculation of transfer reactions within the adiabatic wave approximation. Luke Titus is funded partly by NNSA and partly by NSF.

- Nunes was involved in the interpretation of the GRETINA data taken at NSCL to study ^{56}Ni(d,n)^{57}Cu (manuscript in preparation).

- Nunes collaborated with Fred Sarazin from Colorado (and his former student Duane Smalley) on the analysis of TRIUMF data for the reaction ^{12}C(^{6}He,^{4}He)^{14}C, as well as the writing of the paper [28].

- Nunes collaborated with Kate Jones from University of Tennessee (and her former student Kyle Schmitt) on the analysis of the ORNL data on ^{10}Be(d,p)^{11}Be, as well as the writing of the paper [27].

Elster and others at OU

- In the context of microscopical optical potentials, Elster, Weppner and Ph.D. student A. Orazbayev finished their work on open shell effects in a microscopic optical potential for elastic scattering ^{6}He and ^{8}He. In this work elastic scattering observables (differential cross section and analyzing power) are calculated for the reaction ^{6}He(p,p)^{6}He at projectile energies starting at 71 MeV/nucleon. The optical potential needed to describe the reaction is based on a microscopic Watson first-order folding potential, which explicitly takes into account that the two neutrons outside the ^{4}He-core occupy an open p-shell. The folding of the single-particle harmonic oscillator density matrix with the nucleon-nucleon t-matrix leads for this case to new terms not present in traditional folding optical potentials for closed shell nuclei. The findings of this work are published in *Physical Review C* [24].

- Elster, Phillips and former graduate student C. Ji (now at TRIUMF) collaborate on a lowest order calculation in 'Halo Effective Field Theory' to obtain the ground state of ^{6}He in a three-body Faddeev formulation. A manuscript is in preparation.

2.4 Capture Reactions

G. Arbanas, I.J. Thompson, and J. Escher

2.4.1 Neutron capture on deformed nuclei

Over the past two years of this collaboration we have considered contributions to direct capture coming from two-step processes, like capture via giant-dipole resonances or the isobaric analogue resonances. Although we plan to continue to pursue these venue, this year we focused on a problem

that affects treatments of the direct capture on non-spherical (deformed) nuclei. Models of direct capture of neutrons have so far accounted for the effects of deformed nuclei either in the incoming wave functions (via non-spherical optical model potentials)[23], *or* in the final bound states (via non-spherical real potential wells)[2, 18], but not in both. Since it is known that a spherical optical potentials do not give a good reproduction of low energy neutron-scattering observables of deformed nuclei, we considered it worthwhile to perform a calculation in which the initial and final states are both treated in a self-consistent, deformed-nucleus picture. We have done this in the coupled-channels model of nuclear reactions implemented in the FRESCO code [29] by using the same deformation in the incoming *and* the final state configurations.

We apply this model to neutron capture cross section on Fe-56, that is one of the important structural material nuclides being evaluated by the Collaborative International Evaluated Library Organisation Pilot Project (CIELO[1]) collaboration in order to connect to this high-profile nuclear data initiative and ENDF and USNDP nuclear data programs. We quantify the effect of the non-spherical nuclear shape on the computed direct capture cross section on Fe-56 by comparing to the results for a spherical Fe-56 calculation. We show the results for the incoming neutron energies below 20 MeV for the Koning-Delaroche optical model potential in Fig. 8, and also perform corresponding computations for a real part of this potential.

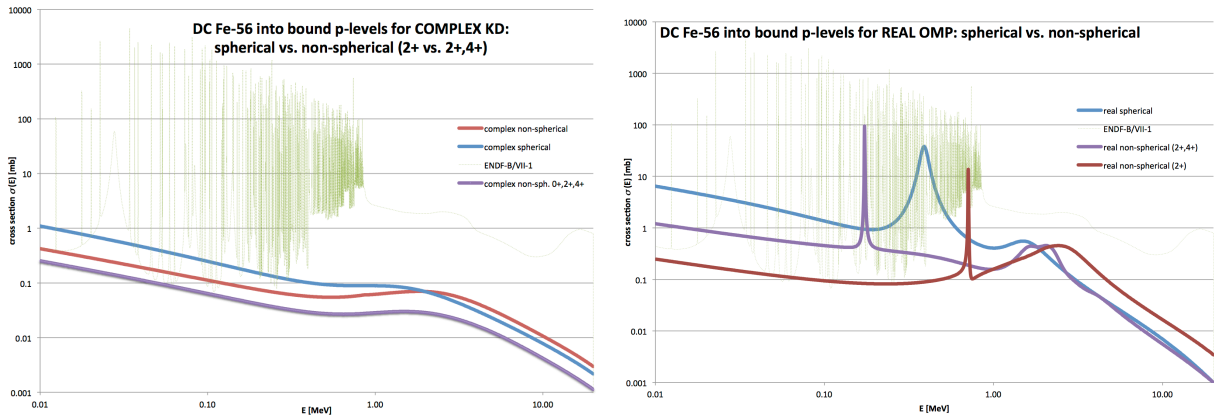

Figure 8: The effect of accounting for nuclear deformation (via coupling to the lowest 2+, 4+ states of the ^{56}Fe rotational band) on computed direct capture cross section is shown by comparison of plots of direct capture on a spherical ^{56}Fe nucleus (blue line), on a deformed ^{56}Fe nucleus (induced by coupling to the first 2+ excited state) (red line), and on a more deformed ^{56}Fe nucleus (induced by coupling to the the first 2+, 4+ excited states) (purple line). The evaluated data from the U.S. ENDF-B/VII.1 (green line), that includes contributions from both direct and resonant cross section, is also shown; the envelope defined by its minima between resonances at low energies could be used to represent the upper limit for direct capture.

In the incoming partition we couple the elastic channel with the two lowest members of the rotational band, the 2^+ excited state at 846 keV and the 4^+ in 2,0851 keV of Fe-56, using a deformation parameter of $\beta_2 = 0.24$ from the RIPL-3 database value extracted by Raman from the B(E2) decay matrix element for both 2+ and 4+ states. We calculated the cross sections to 20 p-wave final bound states with binding energies from 7.65 to 2.61 MeV. The wave functions for the bound states were found using a binding potential that was deformed by the same deformation

[1]https://www.oecd-nea.org/science/wpec/sg40-cielo/

parameter as for scattering. The overall normalization of the bound states was set using the spectroscopic factors from Sen Gupta et al., Nucl. Phys. A160 (1971) 529. We calculated all the E1 transitions from scattering to bound states.

We use the Koning-Delaroche (KD) potential as the spherically-symmetric potential to which the coupling to the rotational band described in the previous paragraph is added. A comparison to the evaluated nuclear data file ENDF-B/VII.1 at low energies shows that only the KD potential with couplings to both 2+ and 4+ yields direct capture that is physically reasonable, i.e. that is smaller than the minima between the resonances of the cross section. A conventional computation of direct capture using KD potential that assumes spherical symmetry overpredicts the data. In any case the magnitude of the effect plotted in Fig. 8 shows the importance of accounting for non-spherical shapes.

To address the uncertainty about use of complex optical potentials to model reactions below 100 keV instead of pure real potentials, we have also performed a set of corresponding computations for the real component of the Koning-Delaroche potential. We find that even with added couplings to the rotational band the computed direct capture over predicts the data.

Computations performed using the (complex) Koning-Delaroche optical model potential plotted on the left side of Fig. 8, show that coupling to 2+,4+ states brings the DC below the minima of the ENDF cross section. This is not the case for computations using the real part of KD only plotted on the right side of Fig. 8, where DC is greater than the minima of ENDF data at low energies. It is hoped that accounting for the missing physics would take DC below ENDF minima at low energies even for a real potential. The (complex) KD potential yields results consistent with evaluated data. (Since we are concerned with direct capture, we are not addressing the prominent single-particle resonances apparent for a real potential; these could be projected out by the Wang-Shakin method.) This may imply that use of a purely real potential at low energy reactions must be accompanied by explicit accounting for any overlooked processes, like those via doorway states. We will therefore continue our efforts from previous years to model doorway states effects on the capture (and other) reactions.

2.4.2 Other capture research

- Within a fruitful collaboration between TORUS and the ORNL's Experimental Nuclear Astrophysics Group we have recently started working with Brett Manning (a graduate student for Jolie Cizewski at Rutgers University), on computation of neutron capture cross sections on even tin isotopes ^{124,126,128}Sn. Brett has extracted single-particle spectroscopic factors from (d,p) measurements he performed at the ORNL over the previous 2.5 years. This work is the continuation of similar work we have already performed for ^{130,132}Sn and other nuclides.

- During 2013 we had a lengthy correspondence with Rituparna Kanungo (Saint Mary's University) about the ^{63}Ni(d,p) measurement planned at TRIUMF, that was to complement the recent nTOF's measurement of ^{63}Ni(d,γ). We observed that that computations of direct-capture in this mass range may be unreliable, and that narrow compound p-wave resonances in the capture cross section are a significant contributor to the stellar Maxwellian-averaged cross sections.

- Arbanas is initiating a complementary collaboration with Nicolas Michel, Marek Płoszajczak, and Y. Jaganathen of GANIL, France, to attempt computations of neutron capture cross sections in the framework of the Gamow Shell Model for isotopes near doubly-closed shell nuclei. This work will investigate contributions of many particle-hole components components of resonant and bound states to the capture cross section. This work will be funded by the ORNL's Small SEED Money Fund, while FUSTIPEN grant may pay for travel to GANIL.

3 Project Management

Coordination

- The coordinating P.I. coordinates the different sub-projects, and ensures the cohesion of the overall project.
- Monthly conference calls ensure that practical information is exchanged, and that research projects, visitors and collaborations are properly coordinated.
- Additional conference calls are set up as needed, and our website (see below) is used to deposit internal documents for discussion.
- Collaborative visits and small-group conference calls held on a regular basis to allow for detailed discussions of physics issues.

Website

We have developed a website at http://www.reactiontheory.org that is hosted at MSU. For the public, this site contains general information about our collaboration, our research papers and talks, the workshops and conferences we attend, and lists of relevant experiments.

For ourselves (protected by a password), we have information about our budget, our plans and deliverables, minutes from our meetings and conference calls, and also a place to deposit internal documents for access by the collaboration.

Collaborative visits in Year 3 Q4 and Year 4 Q1-3

- OU and MSU will continue to work closely with regular meetings
- Our 2014 annual meeting will be at MSU, on June 9-10.

4 Postdoctoral Staff and External Collaborators

TORUS Postdoctoral researcher Dr Neelam Upadhyay

Neelam's works this year focused on the numerical implementation of the momentum-space Coulomb distorted wave representation. As a first task, the implementation of the partial wave Coulomb wave function in momentum space was performed. Next, the Coulomb distorted form factors discussed in Section 2.3.1 were implemented both in Fortran90 and Mathematica, for testing the codes.

Dr. Upadhyay moved onto another postdoc position at Louisiana State University in August 2013, and is now working with Jerry Drayer and his group.

TORUS Postdoctoral researcher Dr Vasily Eremenko

Year 4 report: Dr. Eremenko started as postdoctoral researcher at Ohio University May 1, 2013, after having spent about half year at Texas A&M University, working with A. Mukhamedzhanov on the TORUS (d,p) reaction effort.

Since Dr. Eremenko already had experience with the few-body work of the TORUS collaboration, he immediately could immerse himself in the work at OU. Summarizing, his two major achievements during the last year are,
(a) the numerical realization of partial wave Coulomb wave functions in momentum space,
(b) the development and implementation of a Gelfand-Shilov regularization of the oscillating singularity in momentum integrals over a formfactor function and the Coulomb wave function.

Dr. Eremenko is extremely diligent and careful in his numerical as well as analytical work. Without this trait the collaboration would not have been able to tackle the challenges in the handling the development of a robust computer code to evaluate the momentum space Coulomb wave functions for a large range of Sommerfeld parameters. Currently he takes the lead in the publication for *Computer Physics Communication*, where the collaboration wants to make those Coulomb wave functions in momentum space available for use by other researchers. In addition, his careful work made it possible that we can deliver the proof-of-principle calculation of Coulomb distorted formfactors for nuclei from ^{12}C to ^{208}Pb, which is necessary to for developing the (d,p) reaction code according to the formal development of A. Mukhamedzhanov valid for light as well as heavy nuclei. We are in the process of finalizing a publication describing the details of our calculations.

After the successful proof-of-principle demonstration that Coulomb distorted form factors can be calculated for charges as high a $Z = 82$, Dr. Eremenko will take the lead in the development of the (d,p) reaction code based on Faddeev techniques, which the collaboration proposed.

Dr. Eremenko is hired on the DOE Nuclear Theory grant at Ohio University starting September 1, 2014. His appointment will end August, 31, 2015. The additional funds supplementing the TORUS grant at Ohio University are intended to support Dr. Eremenko in the months June, July, and August 2014, so that the (d,p) reaction work at Ohio University can progress without interruption.

Ohio University doctoral student Mr Linda Hlophe

Year 4 report: The TORUS grant supported Ohio University graduate student Linda Hlophe during the Spring quarter 2012, and the Spring semester 2013. After this he was and currently is supported by the DOE contract No. DE-FG02-93ER40756 with Ohio University.

Linda Hlophe developed the separable representation of n+nucleus optical potentials for ^{12}C, ^{48}Ca, ^{132}Sn, and ^{208}Pb. This work appeared in Physical Review C in the December issue. Following his n+nucleus work, Linda concentrated on the separable optical potentials for p+nucleus, i.e. providing the nuclear formfactor which were used by Dr. Eremenko to calculate Coulomb distorted formfactors. He reworked his codes in more general terms, so that they can take any EST formfactor and calculate the corresponding separable optical potential. By this, the modifications, which have to occur for p+nucleus scattering are automatically included. Linda further developed the code to compute S-matrix elements and p+nucleus phase shifts, so that the partial wave s-matrix elements (and phase shifts) calculated with the separable potential computed with Coulomb distorted form factors can be compared to exact calculations made by FRESCO. This work was more involved than initially anticipated, thus it will also be part of Linda Hlophe's Ph.D. thesis.

Furthermore, Linda Hlophe decided to stay with the TORUS collaboration for his remaining thesis work. He will develop the separable coupling potentials needed to add the transfer to resonances or bound states with a small binding energy, needed in the development of a Faddeev based (d,p) reaction code. The funds for supporting Linda Hlophe in Spring semester 2015 is at present not secured.

Linda Hlophe defended his Ph.D. prospectus containing this future aspect of his work in November 2014.

External Visitors in Year 3 Q4 and Year 4 Q1-3

- Ron Johnson (Surrey) visited Nunes at MSU during May 2013. During that period the group from OU came to MSU for a two day meeting, for discussions on various topics including the work on the EST separable potentials [16].
- The grant contributed to one visits of Prof. Stephen Weppner (Summer 2013) for collaboration on the separable representation of his phenomenological optical potential as well as on the microscopic optical potential for ^{6}He and ^{8}He.

Other Collaborators in Year 3 Q4 and Year 4 Q1-3

These collaborations contributed to our project, but were not funded by this grant:

- F.S. Dietrich (LLNL) and A.K. Kerman (MIT/ORNL)

Planned Visitors in Year 4 Q4 and Year 5

We plan to support the visits of the following people in Year 5 as visitors or consultants:

- Dr. Arnas Deltuva collaborating with Nunes, Elster, and Eremenko on Faddeev techniques for (d,p) reactions using separable potentials.

5 Plans for Year 5

1. Implementation of the AGS equations in the distorted Coulomb basis, with Eremenko and Elster leading this project. Nunes will continue to collaborate.

2. Inclusion of core excitation in the EST formulation for separable optical potentials: Elster will provide guidance to Hlophe (student in OU) with additional guidance from Nunes. It will be part of Hlophe's PhD thesis.

3. Learning from previous AGS implementations: Given the extended experience of Deltuva in implementing AGS equations, Nunes will continue to collaborate with Deltuva, to bring his invaluable knowhow to our collaboration (visit is planned later in 2014).

4. Calculate transfer cross sections using the newly-implemented surface-operator with initial CDCC wave functions by Thompson and Escher, to determine surface and breakup contributions.

5. Arbanas, Thompson and Escher will develop the necessary new semi-microscopic methods to treat doorway states in neutron scattering and capture, and apply it to select nuclides. We will extend FRESCO to account for E2 core transitions for improved computations of direct-capture.

6 Deliverables

6.1 Publications

1. Published paper [15]: Phys. Rev C **88**, 064608(11 Dec 2013)
   Separable Representation of Phenomenological Optical Potentials of Woods-Saxon Type, L. Hlophe, Ch. Elster, R.C. Johnson, N.J. Upadhyay, F.M. Nunes, G. Arbanas, V. Eremenko, J.E. Escher, and I.J. Thompson,
   Background: One important ingredient for many applications of nuclear physics to astrophysics, nuclear energy, and stockpile stewardship are cross sections for reactions of neutrons with rare isotopes. Since direct measurements are often not feasible, indirect methods, e.g. (d,p) reactions, should be used. Those (d,p) reactions may be viewed as three-body reactions and described with Faddeev techniques. Purpose: Faddeev equations in momentum space have a long tradition of utilizing separable interactions in order to arrive at sets of coupled integral equations in one variable. While there exist several separable representations for the nucleon-nucleon interaction, the optical potential between a neutron (proton) and a nucleus is not readily available in separable form. The purpose of this paper is to introduce a separable representation for complex phenomenological optical potentials of Woods-Saxon type. Results: Starting from a global optical potential, a separable representation thereof is introduced based on the Ernst-Shakin-Thaler (EST) scheme. This scheme is generalized to non-hermitian potentials. Applications to n+48Ca, n+132Sn and n+208Pb are investigated for energies from 0 to 50 MeV and the quality of the representation is examined. Conclusions: We find a good description of the on-shell t-matrix for all systems with rank up to 5. The required rank depends inversely on the angular momentum. The resulting separable interaction exhibits a different off-shell behavior compared to the original potential, reducing the high momentum contributions.
2. Published paper [9]: Few-Body Systems 2013, DOI: 10.1007/s00601-013-0644-y
   Microscopic Optical Potentials for Helium-6 scattering off Protons,
   Ch. Elster, A. Orazbayev, S.P. Weppner.
   The 20th International IUPAP Conference on Few-Body Problems in Physics, August 20-25, 2012, Fukuoka, Japan.
   The differential cross section and the analyzing power are calculated for elastic scattering of ^{6}He from a proton target using a microscopic folding optical potential, in which the ^{6}He nucleus is described in terms of a ^{4}He-core with two additional neutrons in the valence p-shell. In contrast to previous work of that nature, all contributions from the interaction of the valence neutrons with the target protons are taken into account.
3. Published monograph chapter [30]: '50 Years of Nuclear BCS', Eds. R.A. Broglia and V. Zelevinsky, World Scientific (2013).
   Reaction mechanisms of pair transfer, I.J. Thompson
   The mechanisms of nuclear transfer reactions are described for the transfer of two nucleons from one nucleus to another. Two-nucleon overlap functions are defined in various coordinate systems, and their transformation coefficients given between coordinate systems. Post and prior couplings are defined for sequential transfer mechanisms, and it is demonstrated that the combination of 'prior-post' couplings avoids non-orthogonality terms, but does not avoid couplings that do not have good zero-range approximations. The simultaneous and sequential mechanisms are demonstrated for the ^{124}Sn(p,t)^{122}Sn reaction at 25 MeV using shell-model overlap functions. The interference between the various simultaneous and sequential amplitudes is shown.
4. Published paper [26]: Phys. Rev C **88**, 031301(R) (2013).
   Remnants of spherical shell structures in deformed nuclei: The impact of an N = 64

neutron subshell closure on the structure of N $\simeq$ 90 gadolinium nuclei, T.J. Ross, R.O. Hughes, C.W. Beausang, J.M. Allmond, C.T. Angell, M.S. Basunia, D.L. Bleuel, J.T. Burke, R.J. Casperson, J.E. Escher, P. Fallon, R. Hatarik, J. Munson, S. Paschalis, M. Petri, L.W. Phair, J.J. Ressler, and N. D. Scielzo,

Odd-mass gadolinium isotopes around N=90 were populated by the (p,d) reaction, utilizing 25-MeV protons, resulting in population of low-spin quasineutron states at energies near and below the Fermi surface. Systematics of the single quasineutron levels populated are presented. A large excitation energy gap is observed between levels originating from the 2d3/2, 1h11/2, and 3s1/2 spherical parents (above theN=64 gap), and the 2d5/2 (below the gap), indicating that the spherical shell model level spacing is maintained at least to moderate deformations.

5. Published paper [24]: Phys. Rev C **88**, 034610 (2013).
   Open Shell Effects in a Microscopic Optical Potential for Elastic Scattering of $^{6(8)}$He, A. Orazbayev, Ch. Elster, S.P. Weppner,

   Elastic scattering observables (differential cross section and analyzing power) are calculated for the reaction 6He(p,p)6He at projectile energies starting at 71 MeV/nucleon. The optical potential needed to describe the reaction is based on a microscopic Watson first-order folding potential, which explicitly takes into account that the two neutrons outside the 4He-core occupy an open p-shell. The folding of the single-particle harmonic oscillator density matrix with the nucleon-nucleon t-matrix leads for this case to new terms not present in traditional folding optical potentials for closed shell nuclei. The effect of those new terms on the elastic scattering observables is investigated. Furthermore, the influence of an exponential tail of the p-shell wave functions on the scattering observables is studied, as well as the sensitivity of the observables to variations of matter and charge radius. Finally elastic scattering observables for the reaction 8He(p,p)8He are presented at selected projectile energies.
6. **Reactions of a ^{10}Be beam on proton and deuteron targets**, K.T. Schmitt et al., Phys. Rev. C 88, 064612, (2013).
7. **Two-neutron transfer reaction mechanisms for ^{12}C(^{6}He,^{4}He)^{14}C using a realistic 3-body ^{6}He model**, D. Smalley et al, Phys. Rev. C 89, 024602 (2014).
8. **Microscopic Optical Potentials for Helium-6 Scattering off Protons**, Ch. Elster, A. Orazbayev, S.P. Weppner, Few Body Syst. **54**, 1399 (2013).
9. **Two-Nucleon Scattering without partial waves using a momentum space Argonne V18 interaction**, S. Veerasamy, Ch. Elster, W.N. Polyzou, Few-Body Syst. **54**, 2207 (2013).

6.2 Papers submitted

1. **Coulomb in momentum space without screening**, N.J. Upadhyay, V. Eremenko, L. Hlophe, F.M. Nunes, Ch. Elster, G. Arbanas, J.E. Escher, and I.J. Thompson (TORUS Collaboration), Phys. Rev. C.
2. **Nuclear Theory and Science of the Facility for Rare Isotope Beams**, A.B Balantekin, J. Carlson, D.J. Dean, G.M. Fuller, R.J. Furnstahl, M. Hjorth-Jensen, R.V.F. Janssens, Bao-An Li, W. Nazarewicz, F.M. Nunes, W.E. Ormand, S. Reddy, B.M. Sherrill, Phys. Lett. A
3. **Coupled-channel treatment of Isobaric Analog Resonances in (p,pγ) Capture Processes**, I.J. Thompson, and G. Arbanas, Nuclear Data Sheets.
4. **Coupled-Channel Models of Direct-Semidirect Capture via Giant-Dipole Resonances**, I.J. Thompson, J.E. Escher, and G. Arbanas, Nuclear Data Sheets

5. **Revisiting Surface-Integral Formulations for One-Nucleon Transfers to Bound and Resonance States**, J.E. Escher, I.J. Thompson, G. Arbanas, Ch. Elster, V. Eremenko, L.Hlophe, F.M. Nunes, N.J. Upadhyay, Phys. Rev. C.
6. **Testing the Perey effect**, L. Titus and F.M. Nunes, Phys. Rev. C.
7. **^{236}Pu(n,f), ^{237}Pu(n,f) and ^{238}Pu(n,f) cross sections deduced from (p,t), (p,d) and (p,p?) surrogate reactions**, R.O. Hughes, C.W. Beausang, T. J. Ross, J.T. Burke, R.J. Casperson, N. Cooper, J.E. Escher, K. Gell, E. Good, P. Humby, M. McCleskey, A. Saastimoinen, T.D. Tarlow, and I.J. Thompson, Phys. Rev. C.

6.3 Presentations

1. *Theory for Low-Energy Nuclear Reactions*, Invited Lectures by Jutta Escher at the "Exotic Beam Summer School 2013," Lawrence Berkeley National Laboratory, Berkeley, CA, July 29 - August 3, 2013.
2. *Theory for Low-Energy Nuclear Reactions*, Invited Lectures by Jutta Escher at UC Berkeley, Berkeley, CA, November 4 & 6, 2013.
3. *Towards an Improved Understanding of the Formation and Decay of Compound Nuclei*, Invited Conference Talk by Jutta Escher at the *4th International Workshop on Compound-Nuclear Reactions and Related Topics (CNR*13)*, Maresias, Brazil, October 7-11, 2013.
4. *Lectures on Reaction Theory*, Invited Lectures by Filomena Nunes, TALENT course 6, Caen, 1-20 July 2013
5. *Overview of Nuclear Theory*, Invited Talk by Filomena Nunes, Physics of Atomic Nuclei Program, East Lansing, August 2013
6. *Updates on FRIB and FRIB theory*, Invited Talk by Filomena Nunes, NUCLEI collaboration meeting, Bloomington, June 2013
7. *Theoretical developments in the study of deuteron induced reactions*, Invited Talk by Filomena Nunes, Nuclear structure and reactions: EXperimental and Ab-initio theoretical perspectives, 18-21 Feb 2014
8. *Quantifying the limits of the (d,p) reaction theories* Interview Talk by Neelam Upadhyay, National Superconducting Cyclotron Laboratory, Michigan State University, East Lansing, 28 February 2013
9. *The (d,p) reaction theories & their limitations* Interview Talk by Neelam Upadhyay, Department of Physics Astronomy, Louisiana State University, Baton Rouge, 8 March 2013
10. *Limitations of (d,p) reaction theory* Talk by Neelam Upadhyay, Stewardship Science Academic Alliance (SSAA) Meeting, Lawrence Livermore National Laboratory, Livermore, 18-19 March 2013
11. *Methods for Vertex Integrals of Coulomb Potentials* Talk by Neelam Upadhyay, TORUS Third Year Review, Lawrence Livermore National Laboratory, Livermore, 11-12 June 2013
12. Annual Meeting of the Division of Nuclear Physics (DNP), October 24-26, Newport News, VA, 'Coulomb distorted nuclear matrix elements in momentum space: I. Formal aspects', N.J. Upadhyay, V. Eremenko, L. Hlophe, F.M. Nunes, Ch. Elster.
13. Annual Meeting of the Division of Nuclear Physics (DNP), October 24-26, Newport News, VA, Coulomb distorted nuclear matrix elements in momentum space: II. Computational Aspect, V. Eremenko, N.J. Upadhyay, L. Hlophe, Ch. Elster, F.M. Nunes.

14. Annual Meeting of the Division of Nuclear Physics (DNP), October 24-26, Newport News, VA, 'The Similarity Renormalization Group for the Three-Body Bound State: A Three-Dimensional Approach', M. Hadizadeh, K. A. Wendt, Ch. Elster.
15. The 22nd European Conference on Few-Body Problems in Physics, September 9-13, 2013, Krakow, Poland, 'Momentum Space Coulomb Distorted Matrix Elements for Heavy Nuclei', Ch. Elster, V. Eremenko, N.J. Upadhyay, L. Hlophe, F.M. Nunes, G. Arbanas, J.E. Escher, I.J. Thompson.
16. 26th Midwest Nuclear Theory Get-Together, Sept. 6-7, 2013, Argonne, IL, 'Momentum Space Coulomb Distorted Matrix Elements for Heavy Nuclei', V. Eremenko, N.J. Upadhyay, F.M. Nunes, Ch. Elster, L. Hlophe, G. Arbanas, J.E. Escher, I.J. Thompson (The TORUS Collaboration).
17. International Workshop on Nuclear Dynamics with Effective Field Theories, July 1-3. 2013, Bochum, Germany, 'Towards (d,p) Reactions with Heavy Nuclei in a Faddeev Description', Inv. Talk, Ch. Elster, Proceedings *arXiv:1309.5820 [nucl-th]*.
18. APS April Meeting 2013, April 13-16, Denver, CO, 'Microscopic Optical Potential for Scattering of ^{6}He and ^{8}He off Protons, Ch. Elster, A. Orazbayev, S.P. Weppner.
19. Spring 2013 Meeting of the APS Ohio-Region Section, March 29-30, Athens, Ohio, 'Effect of varying charge and mattter radii on observables in ^{6}He and ^{8}He', A. Orazbayev, Ch. Elster, S.P. Weppner.
20. Spring 2013 Meeting of the APS Ohio-Region Section, March 29-30, Athens, Ohio, 'Separabilization of Optical Potentials in Momentum Space', L. Hlophe, Ch. Elster.
21. Panel Session on the Future of Few-Body Physics, B.L.G. Bakker, J. Carbonnell, CH. Elster, E. Epelbaum, N.Kalantar-Nayestanaki, J.-M. Richard, to appear in Few-Body Systems.
22. Towards (d,p) Reactions with Heavy Nuclei in a Faddeev Description, L. Hlophe, Ch. Elster, L. Hlophe, V. Eremenko, N.J Upadhyay, F.M. Nunes, G. Arbanas, J.E. Escher, I.J. Thompson, International Workshop on Nuclear Dynamics with Effective Field Theories, July 1-3. 2013, Bochum, Germany, *arXiv:1309.5820 [nucl-th]*.
23. International Conference on Nuclear Data for Science and Technology, March 4-8, 2013, New York, NY, 'Coupled-channel treatment of Isobaric Analog Resonances in (p,pγ) Capture Processes', I.J. Thompson, and G. Arbanas, to appear in Nuclear Data Sheets.
24. International Conference on Nuclear Data for Science and Technology, March 4-8, 2013, New York, NY, 'Coupled-Channel Models of Direct-Semidirect Capture via Giant-Dipole Resonances', I.J. Thompson, J.E. Escher, and G. Arbanas, to appear in Nuclear Data Sheets.
25. NEMEA-7/CIELO International Collaboration on Nuclear Data A workshop of the Collaborative International Evaluated Library Organisation, November 5-8, 2013, Geel, Belgium, 'A self-consistent coupled-channels method for direct neutron capture on non-spherical nuclei: ^{56}Fe(n,γ)^{57}Fe', I.J. Thompson, G. Arbanas, J. Escher, C. Elster, and F.M. Nunes.
26. Nuclear Data Week: USNDP/CSEWG/NDAG Meetings, Nov 18-22, 2013, Brookhaven National Laboratory, NY, 'Direct Capture Reactions', G. Arbanas, I.J. Thompson, J.E. Escher, F.S. Dietrich.

References

[1] N. Austern, Y. Iseri, M. Kamimura, M. Kawai, G. Rawitscher, and M. Yahiro, *Continuum-discretized coupled-channels calculations for three-body models of deuteron-nucleus reactions*, Phys. Rep., **154** (1987), pp. 125–204.

[2] J. P. Boisson and S. Jang, *Direct and Semi-Direct Capture of Nucleons in Deformed Nuclei*, Nuclear Physics A, **A189** (1972), pp. 334–352.

[3] A. Deltuva, *Faddeev-type calculation of three-body nuclear reactions including core excitation*, Phys. Rev. C, **88** (2013), p. 011601.

[4] A. Deltuva and A. Fonseca, *Three-body Faddeev-Alt-Grassberger-Sandhas approach to direct nuclear reactions*, Phys.Rev., **C79** (2009), p. 014606.

[5] A. Deltuva, A. Fonseca, and P. Sauer, *Momentum-space description of three-nucleon breakup reactions including the Coulomb interaction*, Phys.Rev., **C72** (2005), p. 054004.

[6] ——, *Momentum-space treatment of Coulomb interaction in three-nucleon reactions with two protons*, Phys.Rev., **C71** (2005), p. 054005.

[7] A. Deltuva, A. M. Moro, E. Cravo, F. M. Nunes, and A. C. Fonseca, *Three-body description of direct nuclear reactions: Comparison with the continuum discretized coupled channels method*, Phys. Rev. C, **76** (2007), p. 064602.

[8] E. Dolinskii and A. Mukhamedzhanov, *Coulomb effects in direct nuclear reactions*, Sov. Jour. Nucl. Phys., **3** (1966), pp. 180–187.

[9] C. Elster, A. Orazbayev, and S. Weppner, *Microscopic optical potentials for helium-6 scattering off protons*, Few-Body Systems, (2013), pp. 1–5.

[10] V. Eremenko et al., *Partial Wave Coulomb Wavefunctions in Momentum Space*, in preparation, (2014).

[11] D. Ernst, C. Shakin, and R. Thaler, *Separable Representations of Two-Body Interactions*, Phys.Rev., **C8** (1973), pp. 46–52.

[12] J. E. Escher, I. J. Thompson, G. Arbanas, C. Elster, V. Eremenko, L. Hlophe, and F. M. Nunes, *Revisiting surface-integral formulations for one-nucleon transfers to bound and resonance states*, submitted to Phys. Rev. C, (2014).

[13] I. Gel'fand and G. Shilov, *Generalized Functions, Vol. 1: Properties and Operations.*, Generalized Functions, Vol. 1: Properties and Operations., (1964).

[14] J. Haidenbauer, Y. Koike, and W. Plessas, *Separable representation of the Bonn nucleon-nucleon potential*, Phys.Rev., **C33** (1986), pp. 439–446.

[15] L. Hlophe, C. Elster, R. C. Johnson, N. J. Upadhyay, F. M. Nunes, G. Arbanas, V. Eremenko, J. E. Escher, and I. J. Thompson, *Separable representation of phenomenological optical potentials of woods-saxon type*, Phys. Rev. C, **88** (2013), p. 064608.

[16] L. Hlophe et al., *Separable Representation of Phenomenological Optical Potentials of Woods-Saxon Type*, Phys.Rev., **C88** (2013), p. 064608.

[17] R. O. Hughes, C. W. Beausang, T. J. Ross, J. T. Burke, R. J. Casperson, N. Cooper, J. E. Escher, K. Gell, E. Good, P. Humby, M. McCleskey, A. Saastimoinen, T. D. Tarlow, and I. J. Thompson, ^{236}*Pu(n,f),* ^{237}*Pu(n,f), and* ^{238}*Pu(n,f) cross sections deduced from (p,t), (p,d), and (p,p′) surrogate reactions*, to be submitted, (2014).

[18] H. Kitazawa, T. Hayase, and N. Yamamuro, *Direct and Collective Captures of Energetic Neutrons by Ellipsoidally Deformed Nuclei*, Nuclear Physics A, **A307** (1978), pp. 1–21.

[19] A. Mukhamedzhanov, V. Eremenko, and A. Sattarov, *Generalized Faddeev equations in the AGS form for deuteron stripping with explicit inclusion of target excitations and Coulomb interaction*, Phys.Rev., **C86** (2012), p. 034001.

[20] A. M. Mukhamedzhanov, *Theory of deuteron stripping: From surface integrals to a generalized R-matrix approach*, Phys. Rev. C, **84** (2011), p. 044616.

[21] A. M. Mukhamedzhanov, V. Eremenko, and A. I. Sattarov, *Generalized faddeev equations in the alt-grassberger-sandhas form for deuteron stripping with explicit inclusion of target excitations and coulomb interaction*, Phys. Rev. C, **86** (2012), p. 034001.

[22] F. Nunes and N. Upadhyay, *Status of reaction theory for studying rare isotopes*, J. Phys. G: Conf. Ser., **403** (2012), p. 012029.

[23] F. M. Nunes, I. Thompson, and R. Johnson, *Core excitation in one neutron halo systems*, Nuclear Physics A, **A596** (1996), p. 171186.

[24] A. Orazbayev, C. Elster, and S. Weppner, *Open Shell Effects in a Microscopic Optical Potential for Elastic Scattering of $^{6(8)}$He*, Phys.Rev., **C88** (2013), p. 034610.

[25] W. Research, *Mathematica, Version 8.0, Champaign, Illinois*, Mathematica, Version 8.0, Champaign, Illinois, (2010).

[26] T. J. Ross, R. O. Hughes, C. W. Beausang, J. M. Allmond, C. T. Angell, M. S. Basunia, D. L. Bleuel, J. T. Burke, R. J. Casperson, J. E. Escher, P. Fallon, R. Hatarik, J. Munson, S. Paschalis, M. Petri, L. W. Phair, J. J. Ressler, and N. D. Scielzo, *Remnants of spherical shell structures in deformed nuclei: The impact of an N = 64 neutron subshell closure on the structure of N$\sim$90 gadolinium nuclei*, Phys. Rev. C, **88** (2013), p. 031301.

[27] K. T. Schmitt, K. L. Jones, S. Ahn, D. W. Bardayan, A. Bey, J. C. Blackmon, S. M. Brown, K. Y. Chae, K. A. Chipps, J. A. Cizewski, K. I. Hahn, J. J. Kolata, R. L. Kozub, J. F. Liang, C. Matei, M. Matos, D. Matyas, B. Moazen, C. D. Nesaraja, F. M. Nunes, P. D. O'Malley, S. D. Pain, W. A. Peters, S. T. Pittman, A. Roberts, D. Shapira, J. F. Shriner, M. S. Smith, I. Spassova, D. W. Stracener, N. J. Upadhyay, A. N. Villano, and G. L. Wilson, *Reactions of a ^{10}Be beam on proton and deuteron targets*, Phys. Rev. C, **88** (2013), p. 064612.

[28] D. Smalley, F. Sarazin, F. M. Nunes, B. A. Brown, P. Adsley, H. Al-Falou, C. Andreoiu, B. Baartman, G. C. Ball, J. C. Blackmon, H. C. Boston, W. N. Catford, S. Chagnon-Lessard, A. Chester, R. M. Churchman, D. S. Cross, C. A. Diget, D. D. Valentino, S. P. Fox, B. R. Fulton, A. Garnsworthy, G. Hackman, U. Hager, R. Kshetri, J. N. Orce, N. A. Orr, E. Paul, M. Pearson, E. T. Rand, J. Rees, S. Sjue, C. E. Svensson, E. Tardiff, A. D. Varela, S. J. Williams, and S. Yates, *Two-neutron transfer reaction mechanisms for ^{12}C(^{6}He,^{4}He)^{14}C using a realistic 3-body ^{6}He model*, Phys. Rev. C, **89** (2014), p. 024602.

[29] I. J. Thompson, *Coupled reaction channels calculations in nuclear physics*, Computer Physics Reports, **7** (1988), pp. 167 – 212.

[30] I. J. Thompson, *Reaction mechanisms of pair transfer*, (2012).

[31] N. Upadhyay, A. Deltuva, and F. Nunes, *Testing the continuum discretized coupled channel method for deuteron induced reactions*, Phys.Rev., **C85** (2012), p. 054621.

[32] N. Upadhyay, V. Eremenko, L. Lholpe, F. Nunes, and C. Elster, Phys. Rev. C, to be submitted, ((2014)).

[33] N. Upadhyay et al., *Coulomb in Momentum Space without Screening*, in preparation, (2014).

[34] R. Varner, W. Thompson, T. McAbee, E. Ludwig, and T. Clegg, *A global nucleon optical model potential*, Phys.Rept., **201** (1991), pp. 57–119.